PERGAMON

Continental Shelf Research 20 (2000) 571–597

CONTINENTAL SHELF RESEARCH

Particulate fluxes and transports on the slope between the southern East China Sea and the South Okinawa Trough

Yu-Chia Chung*, Guo-Wei Hung

Institute of Marine Geology and Chemistry, National Sun Yat-Sen University, Kaohsiung, Taiwan

Abstract

This paper presents time-series variations of the particulate fluxes in resolutions of 3–15 d from 10 mooring sites on the continental slope between the southern East China Sea and the South Okinawa Trough, northeast of Taiwan. Three of these sites were located in a canyon cutting across the slope. Temporal and spatial variations in particulate flux in the study area were strongly affected by the bottom topography, the topographically induced eddies, the intensity of tidal currents, the depth and height above bottom where the traps were deployed, and episodic events. The apparent mass fluxes measured at depths from about 300 to 1350 m at different locations varied with time and showed synchronous variations among the traps deployed at the same site for some sites. The time-averaged mass flux for each individual trap deployed at different depth and in different length of mooring time ranged from 0.77 to 53.7 g m^{-2} d^{-1}. In the canyon the average fluxes were generally greater than 30 g m^{-2} d^{-1} with large standard deviations; at other slope sites the average fluxes were generally less than 10 g m^{-2} d^{-1}, excluding one or two unusually high values which were observed in some individual traps probably reflecting episodic events. The particulate fluxes always increased toward the ocean bottom at each mooring site but the increment was much greater in the canyon. This suggests that the particulates were transported out of the shelf or upper slope area essentially through the canyon where large mass fluxes were observed. The current meter data processed with low-pass filtration and expressed in stick diagrams and progressive vector diagrams showed large temporal and spatial variations which were generally not correlated with those of particulate fluxes. Although strong tidal velocity oscillations in the canyon were found to be associated with high mass fluxes in some instances (Hung and Chung, 1998, Continental Shelf Research 18, 1475–1491), episodic events with very high mass fluxes were generally not related to the current systems. The deduced prevailing flow was consistently along the isobaths of the lower slope toward the southwest even though the current meters were

* Corresponding author. Fax: 8867-525-5150.

E-mail address: ycchung@mail.nsysu.edu.tw (Y.-C. Chung)

0278-4343/00/$ - see front matter
PII: S0278-4343(99)00086-2

deployed in different seasons for variable length of time. The mean current speed varied from 30 cm s^{-1} within the Kuroshio at 305 m depth to 3 cm s^{-1} at about 250 m above the bottom of the deepest site near the South Okinawa Trough. Most values were about 5–10 cm s^{-1}. In contrast to the canyon where the trapped particulates were mostly silt and sand (Hung and Chung, 1998), the particulates collected from the general slope area were mainly silt. High mass fluxes were found to be associated with high sand and silt fluxes in the canyon (Hung and Chung, 1998) probably due to strong tidal currents and episodic events that had occurred in this high-energy environment. Lower mass fluxes with less sand contents observed at general slope sites suggest that no significant amounts of particulates may be transported via the intracanyon areas.

Keywords: Particulate flux; Transport; Current; Continental slope; Canyon; East China Sea; South Okinawa Trough

1. Introduction

As one of the major marginal seas in the world, the East China Sea (ECS) continental shelf receives more than 1.6×10^9 t of particulate matter annually from the Changjiang and the Huanghe rivers (DeMaster et al., 1985). A large portion of these particulates is deposited on the shelf and the remainder may be transported farther away to the slope, the Okinawa Trough, or even to the deep Pacific. The purpose of this study is to delineate the transport pathway and flux of the particulates in the slope area between the southern ECS shelf and the South Okinawa Trough by deployment of both sediment traps and current meters.

The ECS continental shelf is wide in the northeast and narrow in the southwest with its southern end bordering the Taiwan Strait and northern Taiwan. On the shelf, there are the Taiwan Warm Current, a year-round northeast flow roughly parallel to the coast of mainland China, and the Coastal Current which flows along the coast northeastward in summer but southwestward in winter. Along the ECS shelf break, the Kuroshio (the western boundary current of the Pacific) flows northeastward after passing along the east coast of Taiwan (Fig. 1). Part of the Kuroshio water intrudes onto the shelf through the slope area between the North Mien-Hua Canyon and the Mien-Hua Canyon, and generated a cyclonic gyre with a year-round upwelling cold dome off northeast Taiwan (Fan, 1980; Wong et al., 1991; Liu et al., 1992; Tang and Tang, 1994). This intrusion is most intensive in winter when the main axis of the Kuroshio swings toward the mainland, and least intensive in summer when the axis swings toward the open Pacific (Chao, 1990). The intrusion and upwelling of the Kuroshio water induce an intensive exchange and mixing with the Taiwan Warm Current and Coastal Current waters in the study area (Chern and Wang, 1990; Chuang and Wu, 1992). The water on the outer shelf is thus a mixture of these water masses in variable proportions during different seasons. Because of the current pattern and the narrow continental shelf in the southern ECS, the particulate matter on the shelf may be transported through this area and farther into the South Okinawa Trough.

As a component of the Kuroshio Edge Exchange Processes (KEEP, 1989–1994) and Kuroshio–East China Sea Shelf Exchange Processes (KEEP II, 1994–1997) integrated

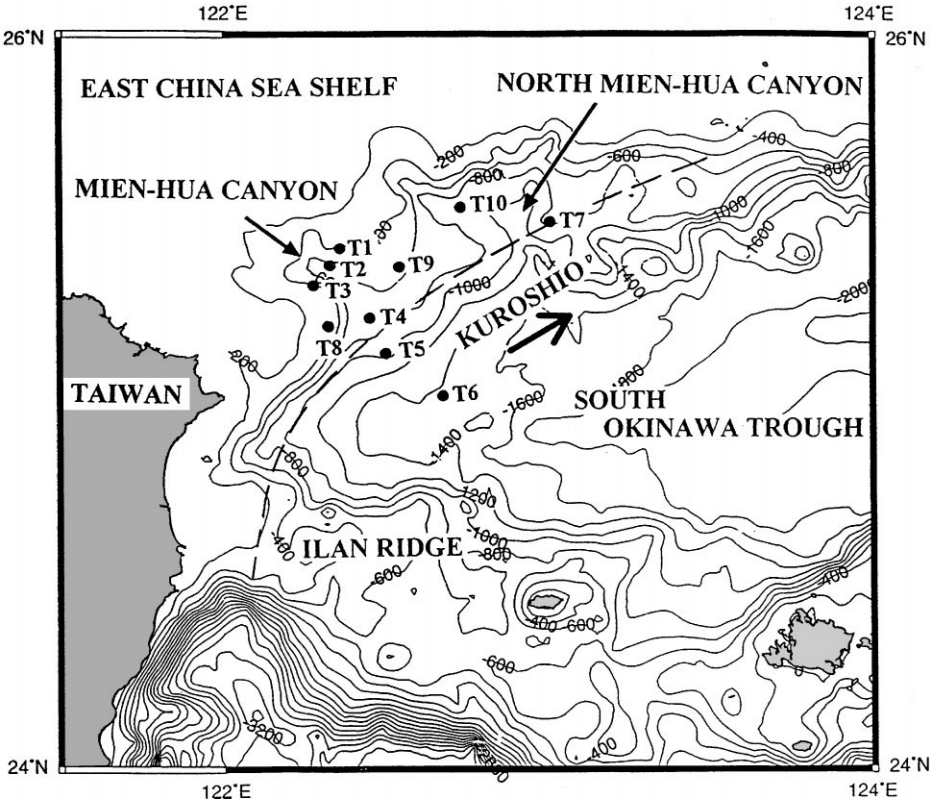

Fig. 1. Map showing locations of the mooring sites for sediment traps and current meters (T1–T10). The Kuroshio path and its rough western margin are indicated, respectively, by a large arrow and a dashed line trending northeast.

programs conducted in Taiwan, time-series sediment traps (PPS 3/3, Heussner et al., 1990) and current meters (Aanderaa, RCM 8) were deployed in, and recovered from the slope area between the southern ECS shelf and the South Okinawa Trough for measurements of particulate fluxes, particle size distributions, compositions, stable isotopes, radionuclides and currents.

This paper presents results on the spatial and temporal variations of the particulate mass fluxes and associated currents obtained from the first 10 mooring sites (designated as T1–T10), the locations of which are shown in Fig. 1 together with major topographic features, the Kuroshio path and its approximate western margin.

2. Methodology

2.1. Traps, preservative and sample handling

The French-made time-series sediment traps PPS 3/3 (Piege a Particules Sequentiel, Model 3/3, a modified version of the PPS 3 used earlier in the French

ECOMARGE (ECOsystemes de MARGE continentale) program) were used in this study. The cylindrical trap with an aspect ratio of 2.5 and a collection area of 0.125 m^2, has a cone at the lower end to funnel the particulates into a collection cup. The trap is equipped with 12 plastic collection cups which are attached to its bottom plate. The collection time of each cup can be preset by the timer. Detailed description of the PPS 3 has been given by Heussner et al. (1990).

The preservative, a buffered formalin solution (5% or $\sim$1.7 M, $7.5 < pH < 8.0$), was a mixture of 37% formaldehyde, some analytical-grade sodium borate and 0.2 μm filtered seawater (taken near the trap deployment location). Each collection cup was filled with the preservative to prevent the trapped particles from degrading (Heussner et al., 1990).

Upon recovery of the traps, the samples were stored in a cold room below 4°C until they were brought back to the laboratory where the supernatant in each sampling cup was transferred by a pipette to an acid-washed plastic vial and stored in a refrigerator at $\sim$ 2°C. After removal of the supernatant, the trapped particles were wet-sieved through 1 mm nylon mesh with 0.2 μm filtered seawater to remove large organisms or debris. The sample was then divided evenly into subsamples by a perimatic dispenser (Jencons Ltd.).

One of the subsamples was filtered with a pre-weighed 47 mm Millipore membrane filter (0.45 μm pore size) and the filtered sample was rinsed with deionized distilled water to remove the sea salt. The desalted sample was dried at $\sim$40°C for 48 h and weighed to determine the mass flux. The sample was then processed for other measurements, such as particle size distributions and radionuclides. The size distributions were determined by a laser particle counter and were expressed in terms of sand, silt and clay fractions. The PPS 3/3 sediment traps, preservatives and sample handling were also briefly described elsewhere (Hung and Chung, 1998).

The remaining subsamples, stored in a refrigerator at $\sim$2°C, were archived and used for other measurements.

2.2. Times and depths deployed

The time-series sediment trap moorings were deployed and recovered from 10 sites (T1–T10) on the ECS continental slope sequentially from October, 1992 to December, 1995. The deployed time and depth of each successful trap are shown in Fig. 2 in which the water depth of each site is also indicated. From T1 to T5, each mooring was deployed in different periods of time with different sampling intervals, while the moorings at T6 and T7 were deployed concurrently with the same sampling intervals. From T8 to T10, all moorings were deployed within the same period with the same sampling intervals. The sampling intervals ranged from 3 d (during the first deployment, T1) to 15 d (T6 and T7). The traps were deployed at depths from about 300 to 1350 m. Information on water depths of the trap sites, moored depths, sampling intervals and moored periods are given in Table 1. The moored depth with brackets indicates failure or malfunction of the trap at that depth.

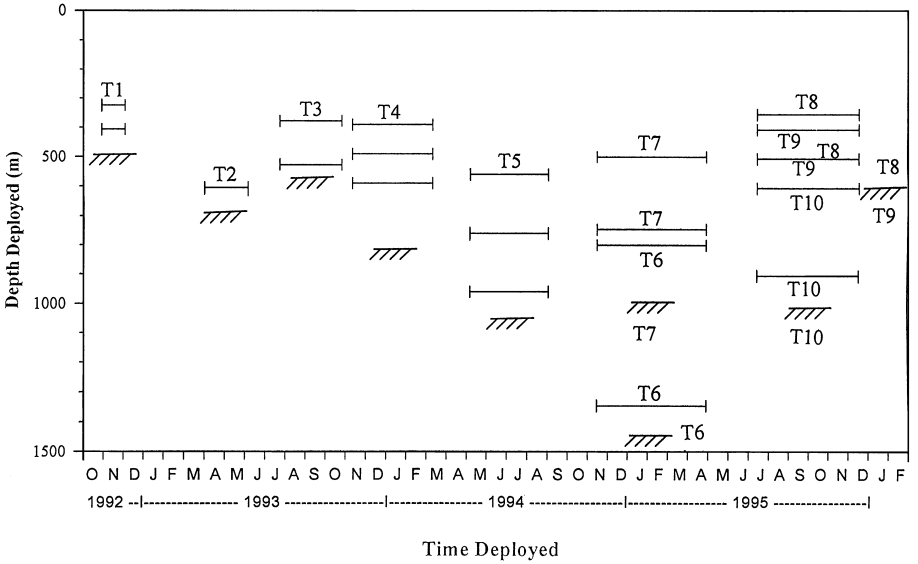

Fig. 2. Deployed depth and time period for sediment trap moorings. The water depth of each mooring site is indicated. Both T8 and T9 are about 600 m deep and are marked to the right side to avoid overlapping on a T10 trap.

2.3. Current meter deployment and data reduction

In order to monitor the flow conditions at each site and depth where sediment traps were deployed, current meters (RCM 8) were deployed usually about 5 m below the traps. In some cases when current meters were in shortage, a current meter was placed at the mid-point between two traps on a mooring string. Most current meters were able to collect data but some failed before the end of the sediment trap mooring due to power failure of the batteries. The depth or height above bottom (mab) of each current meter mooring is given in Table 1. If a current meter failed, the mooring of that current meter was not mentioned. The current meter data were processed and expressed in low-pass filtered stick diagrams and progressive vector diagrams, from which the prevailing direction and mean speed were determined for each deployed depth at each site.

3. Results

3.1. Particulate fluxes

The particulate fluxes determined from the traps deployed at T1–T10 are listed in Table 2. Since the deployment periods and collection time intervals are different for

Table 1
Locations, water depths, moored depths, trap sampling intervals and moored periods for sediment traps and associated current meters at T1–T10 sites[a]

Trap site	Location	Water depth (m)	Moored depth (m) and height (mab)		Sampling interval (d)	Moored period
			Trap	Current meter		
T1	25° 21'N 122° 21'E	490	325 (165) 407 (83)	330 (160) 412 (78)	3	10/27/1992– 12/1/1992
T2	25° 22.4'N 122° 19.1'E	695	[404] 606 (89)	409 (286) 611 (84)	5,6	3/31/1993– 6/4/1993
T3	25° 20.4'N 122° 17.9'E	578	[278] 378 (200) 528 (50)	328 (250) 533 (45)	8	7/21/1993– 10/25/1993
T4	25° 12.6'N 122° 28'E	818	[290] 390 (428) 490 (328) 590 (228)	 395 (423) 595 (223)	10	11/10/1993– 3/9/1994
T5	25° 06.5'N 122° 30.1'E	1060	[360] 560 (500) 760 (300) 960 (100)	365 (695) 565 (495) 765 (295) 965 (95)	10	5/5/1994– 9/1/1994
T6	24° 59.6'N 122° 39.3'E	1446	746 (700) [1046] 1346 (100)	896 (550) 1196 (250)	15	11/14/1994– 5/12/1995
T7	25° 27.4'N 123° 01.6'E	1000	[300] 500 (500) 800 (200)	305 (695) 650 (350)	15	11/14/1994– 5/12/1995
T8	25° 10.1'N 122° 22.1'E	605	355 (250) 505 (100)	360 (245) 510 (95)	13	7/13/1995– 12/15/1995
T9	25° 20.2'N 122° 32.9'E	607	407 (200) 507 (100)	412 (195) 512 (95)	13	7/13/1995– 12/15/1995
T10	25° 30'N 122° 43'E	1006	[306] 606 (400) 906 (100)	 611 (395) 911 (95)	13	7/13/1995– 12/15/1995

[a] *Notes*: [ ] indicates mulfunction of instrument.
( ) indicates meters above bottom (mab).

these moorings (Table 1, Fig. 2), the time-series flux variations are listed in terms of the collection cup number in sequence. There were usually one or two collection cups with extremely high fluxes probably reflecting episodic events; therefore, two

Table 2
Mass flux data in g m^{-2} d^{-1} from sediment traps moored at T1–T10. Locations, moored periods and relevant information are given in Table 1. Variation of the mass fluxes is expressed in terms of the standard deviation from the mean

Trap site	Depth (m)	(mab)	Cup#1	Cup#2	Cup#3	Cup#4	Cup#5	Cup#6	Cup#7	Cup#8	Cup#9	Cup#10	Cup#11	Cup#12	Mean flux[a]	Mean flux[b]
T1	325	165	96.6[c]	23.3	4.6	5.0	61.0	57.6	18.6	5.5	20.0	42.6	22.7	40.0	33.1 ± 27.8	27.4 ± 20.3
	407	83	174.1[c]	41.4	10.5	10.5	54.1	65.5	48.7	18.4	39.9	102.1[c]	52.9	76.2	57.9 ± 45.3	41.8 ± 22.6
T2	606	89	27.8	256.4[c]	27.4	21.5	47.8	47.6	72.5	18.7	17.5	47.8	31.9	40.9	54.8 ± 65.4	36.5 ± 16.7
T3	378	200	12.5	—	2.4	16.0	5.2	5.9	2.9	4.0	4.3	0.4	0.2	2.1	5.1 ± 4.9	
	528	50	60.9	37.7	19.5	181.5[c]	85.2	50.4	38.5	98.5	27.4	37.9	81.1	139.4[c]	71.5 ± 48.9	53.7 ± 26.7
T4	390	428	4.48	1.10	2.96	1.36	2.87	11.61[c]	12.52[c]	4.06	2.38	1.96	1.10	2.15	4.04 ± 3.90	2.43 ± 1.18
	490	328	6.84	2.16	3.69	4.09	3.07	17.25[c]	14.80[c]	5.73	5.94	6.67	1.27	5.03	6.38 ± 4.85	4.45 ± 1.91
	590	228	9.98	4.78	5.03	9.98	7.20	19.02[c]	16.80[c]	7.70	8.04	15.77[c]	4.06	10.48	9.90 ± 4.91	7.47 ± 2.42
T5	560	500	2.03	2.05	10.07[c]	3.22	5.80	3.59	1.73	6.41	3.10	6.64	14.89[c]	5.12	5.39 ± 3.86	3.97 ± 1.88
	760	300	3.05	2.68	8.31[c]	4.63	7.80	7.30	2.90	8.67	5.21	6.15	20.61[c]	15.57[c]	7.74 ± 5.38	5.38 ± 2.25
	960	100	4.68	4.06	14.46[c]	5.67	8.99	8.29	4.07	9.80	9.45	7.26	46.09[c]	36.92[c]	13.31 ± 13.63	6.92 ± 2.34
T6	746	700	3.95	3.42	3.28	5.27	2.61	2.65	3.33	3.48	1.93	2.78	2.97	—	3.24 ± 0.86	
	1346	100	6.74	7.19	7.45	6.45	2.17	2.17	7.28	5.64	3.01	3.30	3.34	—	4.98 ± 2.17	
T7	500	500	0.86	0.92	0.95	—	—	—	—	0.39	1.04	0.85	0.40	—	0.77 ± 0.27	
	800	200	×	4.11	×	3.95	×	2.11	×	2.18	×	2.95	×	×	3.06 ± 0.95	
T8	355	250	13.75	12.74	11.85	3.34	18.33	6.17	15.68	10.98	13.16	18.20	39.17[c]	32.76[c]	16.34 ± 10.22	12.42 ± 4.78
	505	100	35.28	29.13	32.96	13.10	40.69	27.23	37.98	21.95	37.89	39.10	101.2[c]	68.79[c]	40.44 ± 23.32	31.53 ± 8.79
T9	407	200	0.53	0.37	0.73	0.46	0.59	0.49	0.46	1.53	0.69	1.66	1.07	0.69	0.77 ± 0.43	
	507	100	3.31	0.68	2.71	1.59	1.39	1.70	3.00	2.31	1.09	3.49	3.80	7.55[c]	2.72 ± 1.82	2.28 ± 1.05
T10	606	400	1.07	1.02	1.65	1.06	1.94	1.20	1.67	1.57	0.51	0.71	0.86	0.68	1.16 ± 0.45	
	906	100	10.61	7.27	25.61[c]	9.82	21.26[c]	11.16	12.33	5.54	9.73	5.41	7.76	9.75	11.35 ± 6.10	8.94 ± 2.34

[a]Calculated with all data available.
[b]Unusually high values excluded.
[c]Unusually high value relative to others in the same trap.
—: No data.
×: Unusually low or questionable data.

time-averaged mean fluxes are given in Table 2: one calculated with all data, the other without the extremely high values. The mean calculated without the extremely high values is significantly lower than that calculated with all data, and its standard deviation is also much smaller. The mass fluxes obtained from T1 to T3 (in Mien-Hua Canyon) were much higher (except for T3 at 378 m) than those collected from other sites (Table 2). However, the mass fluxes from T8 were quite high and closer to those in the canyon. The data for T1, T2 and T3 are reported to 0.1 g m^{-2} d^{-1} by rounding off 2 digits; the rest are reported to 0.01 g m^{-2} d^{-1} by rounding off 1 digit. The uncertainty of these flux values is estimated to be generally less than 1%, mainly due to very high mass fluxes in the study area.

The temporal variations of the particulate fluxes from T1 to T3 have been discussed (Hung and Chung, 1998). The apparent mass fluxes at different depths from T4 and T5 (Fig. 3) varied periodically and synchronously, and showed higher values at greater depths. The sixth and seventh collection cups (12/30/1993–1/18/1994) of all the three traps at T4 had much higher fluxes (Fig. 3), indicating clearly a synchronized event. At T5, the last two cups (8/13/1994–9/1/1994) of the deeper two traps, especially the deepest one (100 mab), showed extremely high fluxes relative to other cups (Fig. 3), indicating a synchronized episodic event. Fig. 4 shows temporal variations in mass flux from T6 and T7 at the same mooring period, from November 14, 1994 to April 27, 1995. T6, the deepest site located almost within the trough (Fig. 1), had mass flux varying between 2 and 7.5 g m^{-2} d^{-1}. The fluxes of the fifth and sixth cups (1/13/1995–2/11/1995) at the 1346 m trap were lower than those of the corresponding cups at the 746 m trap (Fig. 4). This feature is contradictory to the general trend that mass fluxes at the same site increase with depth at the same collection period. The mass fluxes of these two traps which were separated 600 m apart at T6 showed no synchronous variation. T7 was located within the North Mien-Hua Canyon about 55 km to the northeast of T6 (Fig. 1). The mass fluxes observed at two depths here were generally lower than 4 g m^{-2} d^{-1} (Fig. 4). Although the trapping efficiency could be lowered substantially if the current speed was greater than 12 cm s^{-1} (Baker et al., 1988), these low fluxes were unlikely due to undertrapping caused by the associated currents which were generally lower than 10 cm s^{-1}. This implies that the Kuroshio water has very low particle load before intrusion onto the ECS shelf. There were many cups collecting hardly any particulates at T7. These are not included in Table 2 or plotted in Fig. 4. Although the traps at both T6 and T7 were deployed concurrently at only 55 km apart, the difference in flux variation and magnitude was obvious. No similarity in temporal variation existed probably due to differences in water depth, current pattern and bathymetry. All the mass fluxes measured from T4 to T7 (Figs. 3 and 4) were much lower than those observed within the nearby Mien-Hua Canyon (Table 2).

T8 and T9 were located at about 600 m isobath on the slope to the southwest and northeast of the Mien-Hua Canyon outlet, respectively (Fig. 1). Two traps were deployed at each of the two sites concurrently from July 13 to December 15, 1995 (Table 1, Fig. 2). While the mass fluxes increased with depth at each site as usual but showed only very weak synchronous variation (Fig. 5), the values were an order of magnitude greater at T8 than at T9 (note the scale difference in Fig. 5). The fluxes at

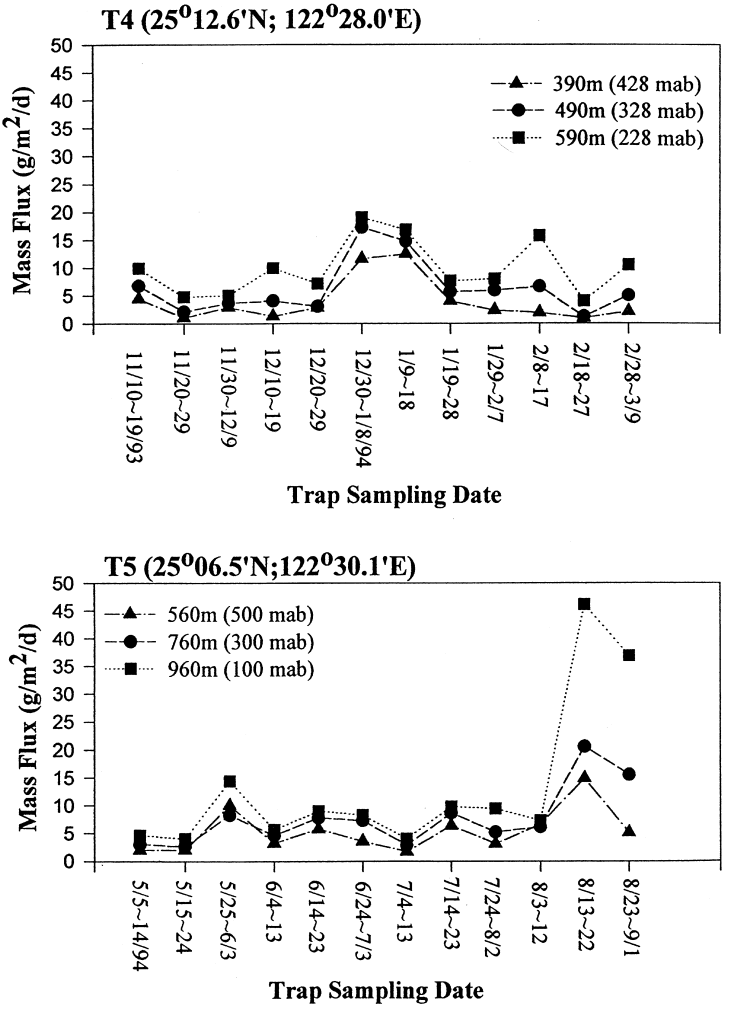

Fig. 3. Temporal mass flux variations at T4 and T5 in a sampling interval of 10 d. Both the deployed depth and height above bottom (mab) are indicated for each trap. Note the difference in sampling dates between T4 and T5. Both T4 and T5 show synchronous time-series variations with greater mass fluxes at greater deployed depths. T5 shows that the episodic event (8/13–22/1994) was recorded concurrently by all three types.

T8 were much higher than those at T4 and T5 nearby but comparable to those at T1, T2 and T3 in the canyon (Table 2). As the current meter data (presented in next subsection) indicated a southwestward flow at both T8 and T9 sites, the high mass fluxes observed at T8 could have been derived from the Mien-Hua Canyon where much higher mass fluxes were observed (Table 2). Thus the particulates may be transported along the isobaths from the canyon outlet toward the southwest. The extremely low mass fluxes observed at T9 imply that particulates may not be

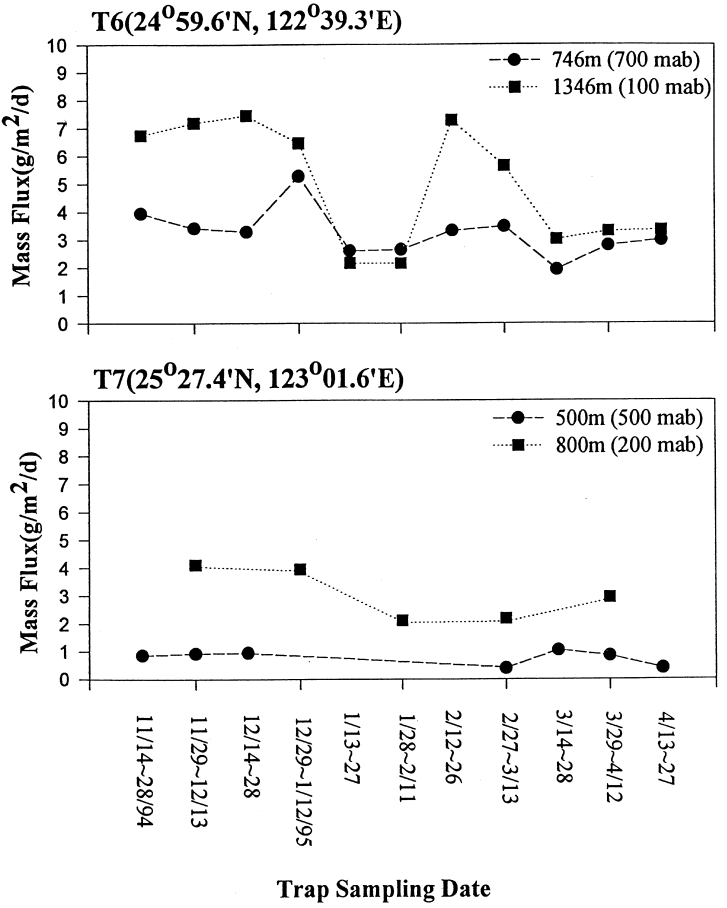

Fig. 4. Temporal mass flux variations at T6 and T7 in a sampling interval of 15 d. Both T6 and T7 were deployed concurrently from November 14, 1994 to April 27, 1995. Questionable data were removed. The mass fluxes were much lower, showing no synchronized temporal variations between traps or sites.

transported across the isobaths at the slope where there is no canyon. The only high mass flux observed at lower trap (100 mab) of T9 from December 3 to 15 appeared to be an episodic event which was not observed 100 m above (Fig. 5). As the mass fluxes were low at T9, the relative abundance of total organic carbon and carbonate was significantly higher due to less dilution by terrigenous materials (Sheu et al., 1999).

T10 was located at the western branch of the North Mien-Hua Canyon (Fig. 1) and deployed concurrently with T8 and T9. The mass fluxes observed at the two traps (606 and 906 m) differed by an order of magnitude (Fig. 5). There were two very high fluxes at the lower trap (100 mab): one from August 8 to 20, the other from September 3 to 15. The temporal variations in mass flux at T10 showed no correlation

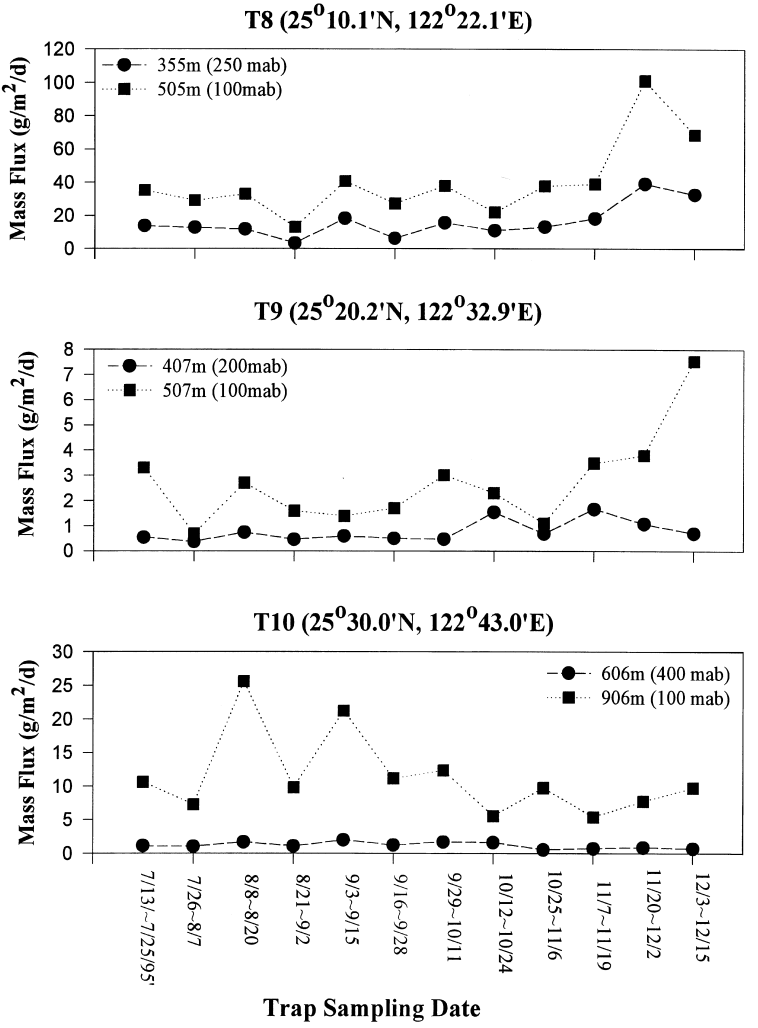

Fig. 5. Concurrent mass flux variations at T8–T10 in a sampling interval of 13 d. Note that different scales are used to accommodate large variations in mass flux observed at different locations. No synchronized temporal variations were observed among these traps and sites.

or synchronized event between the two traps. Although the traps at T8, T9 and T10 were deployed concurrently the temporal variations in mass flux were totally unrelated. Thus the variations appeared to be spatially rather than temporally controlled.

In general, the flux data reported here were higher than those observed in a similar marginal sea environment, such as the submarine canyons off Washington shelf (Baker and Hickey, 1986), the Baltimore Canyon off the east US coast (Gardner, 1989a), the western Gulf of Lions (Monaco et al., 1990) and the SEEP area (Biscaye

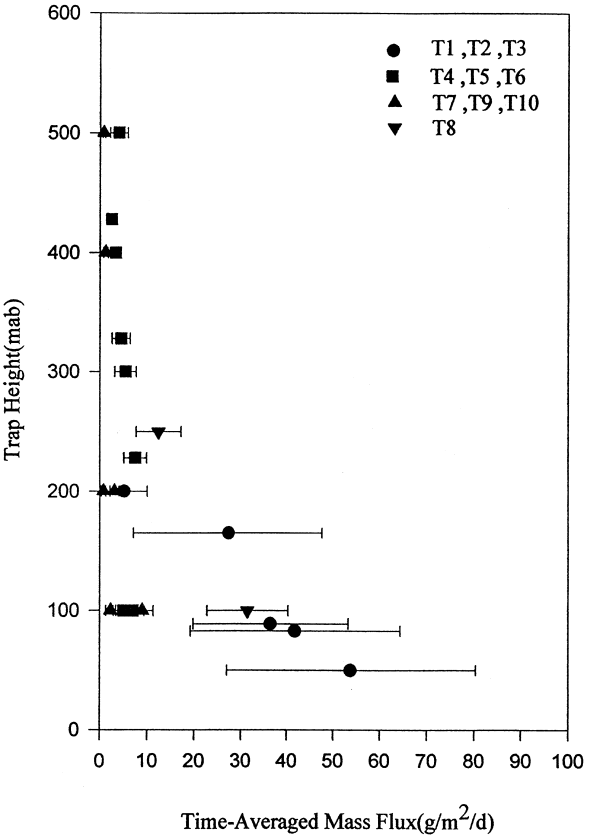

Fig. 6. Plots of the time-averaged mass flux vs. the trap height (meters above bottom, mab). Very high values with large variations were observed within the Mien-Hua Canyon (T1–T3, circle) and at the southwest of the canyon outlet (T8, inversed triangle). Much lower values were observed in the lower slope extending from the Mien-Hua Canyon (T4–T6, square) and other slope areas, including the North Mien-Hua Canyon (T7, T9, T10, triangle).

et al., 1988; Biscaye and Anderson, 1994). Episodic events of relatively very high mass fluxes were also observed in those areas. The time-averaged mass fluxes and their standard deviations from T1 to T10 are plotted against the trap height above the bottom in Fig. 6 despite the facts that the length of time and season of these moorings are different. The plotted mean values are those excluding the extremely high individual mass fluxes (Table 2) so that the episodic events are removed. In the canyon (T1–T3) and the slope southwest of it (T8) the mean values increase toward the bottom with a large increment. Very large standard deviations are often associated with very high mean values of the bottom layer (<200 m) in the canyon. Low mean fluxes (<10 g m^{-2} d^{-1}) obtained from other sites indicate that those waters were relatively "clean". Thus the Mien-Hua Canyon may be a major pathway for particulate transport out of the shelf and upper slope.

3.2. Current meter data

Fig. 7 shows stick diagrams for T4–T7. These diagrams show time-series, low-pass filtered current velocity variations site by site. The direction due north is vertical upward, and the velocity scale is identical for each diagram to allow direct comparison. The calendar dates are labeled for each site. Fig. 7a shows two synchronized time-series stick diagrams for T4: A is at 395 m, and B is at 595 m depth. The current velocities were quite different at the two depths although similarity did occur in some short periods. The maximum velocities were up to 40 cm s^{-1} at 395 m depth while the minimum were below the current meter resolution which was about 1.5 cm s^{-1}. The current velocities were greater at shallower depth.

Fig. 7b shows three sets of stick diagrams for T5 from 365 m (A), 565 m (B) and 765 m (C) depth. No correlation or similarity in current velocities was observed among A, B, and C. The currents at each and all depths had large temporal variations and generally decreased with depth. Maximum velocities of over 30 cm s^{-1} to the southeast were observed at 365 m between June 23 and 28, 1994 but the currents below were quite weak during this period (Fig. 7b). Fig. 7c illustrates data obtained at T6 which is located closest to the South Okinawa Trough with depth over 1000 m. The current velocities were substantially reduced: the maximum was less than 10 cm s^{-1} at 896 m (A) and less than 5 cm s^{-1} at 1196 m (B).

Fig. 7d illustrates data from T7 which is located at the North Mien-Hua Canyon where the Kuroshio intrudes onto the shelf and flows northeastward. Velocities of over 40 cm s^{-1} north- or northeastward were commonly seen at 305 m depth (A). However, the velocities at 650 m (B) were substantially lower, at about 10 cm s^{-1} or less with north- or northwest direction, suggesting a topographic effect on the currents at this depth.

A progressive vector diagram (PVD) is useful in indicating both the major flow direction and the average flow speed. Fig. 8 shows two such diagrams: (A) on top is the PVD from T4 at 595 m; (B) at bottom is the PVD from T8 at 510 m. Both PVDs indicate a southwest flow but with different and variable speed as indicated in the figure. At T4, the speed before December 13, 1993 was relatively fast: about 10.2 km d^{-1} or 12 cm s^{-1}. However, between December 13, 1993 and April 21, 1994, the flow was quite variable even though the overall direction was also toward the southwest. At T8, the southwest flow was relatively uniform or regular with an average speed of about 5.5 km d^{-1} or 6.4 cm s^{-1}. These two sites were very close (about 10 km apart, see Fig. 1) and the PVDs all showed a southwest flow. Thus the particulates were presumably transported toward the southwest in the area. The prevailing flow direction and mean speed as deduced from each current meter data set are given in Table 3. As expected, the mean speed at each site was greater at shallower depth. The maximum at 30 cm s^{-1} was located at T7 (305 m) where a portion of the Kuroshio was flowing through. The values deduced from the lower current meter data sets were generally about 5 cm s^{-1}.

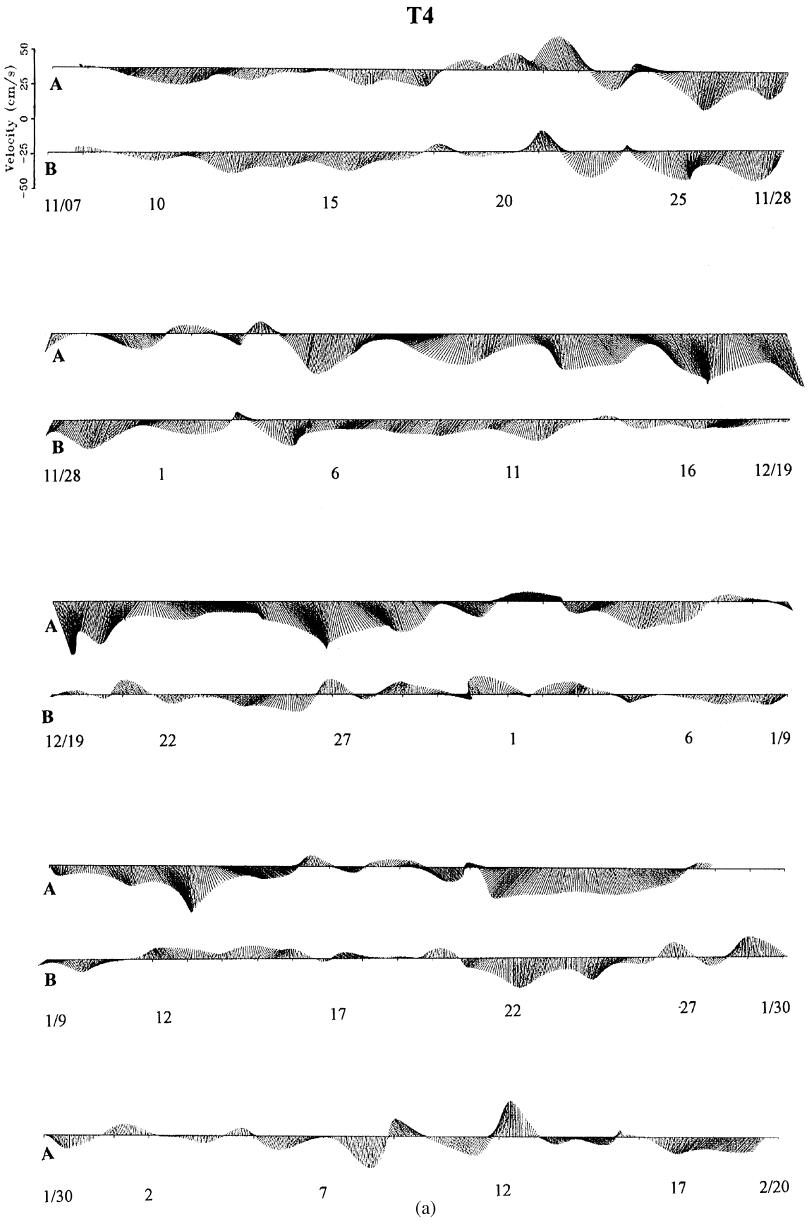

Fig. 7. Stick diagrams showing time-series current velocity (low-pass filtered) variations at T4 (a), T5 (b), T6 (c) and T7 (d). Same velocity scale is used in all diagrams to facilitate easy comparisons. At T4, A represents data from 395 m depth; B from 595 m depth. At T5, A, B and C represent data from 365, 565 and 765 m depth, respectively. At T6, A and B represent data from 896 and 1196 m depth, respectively. At T7, A and B represent data from 305 and 650 m depth, respectively. The general features are: different depths or different layers at the same location had quite different current velocities (in both the direction and magnitude); current velocities were always greater at the upper layers or shallower depths.

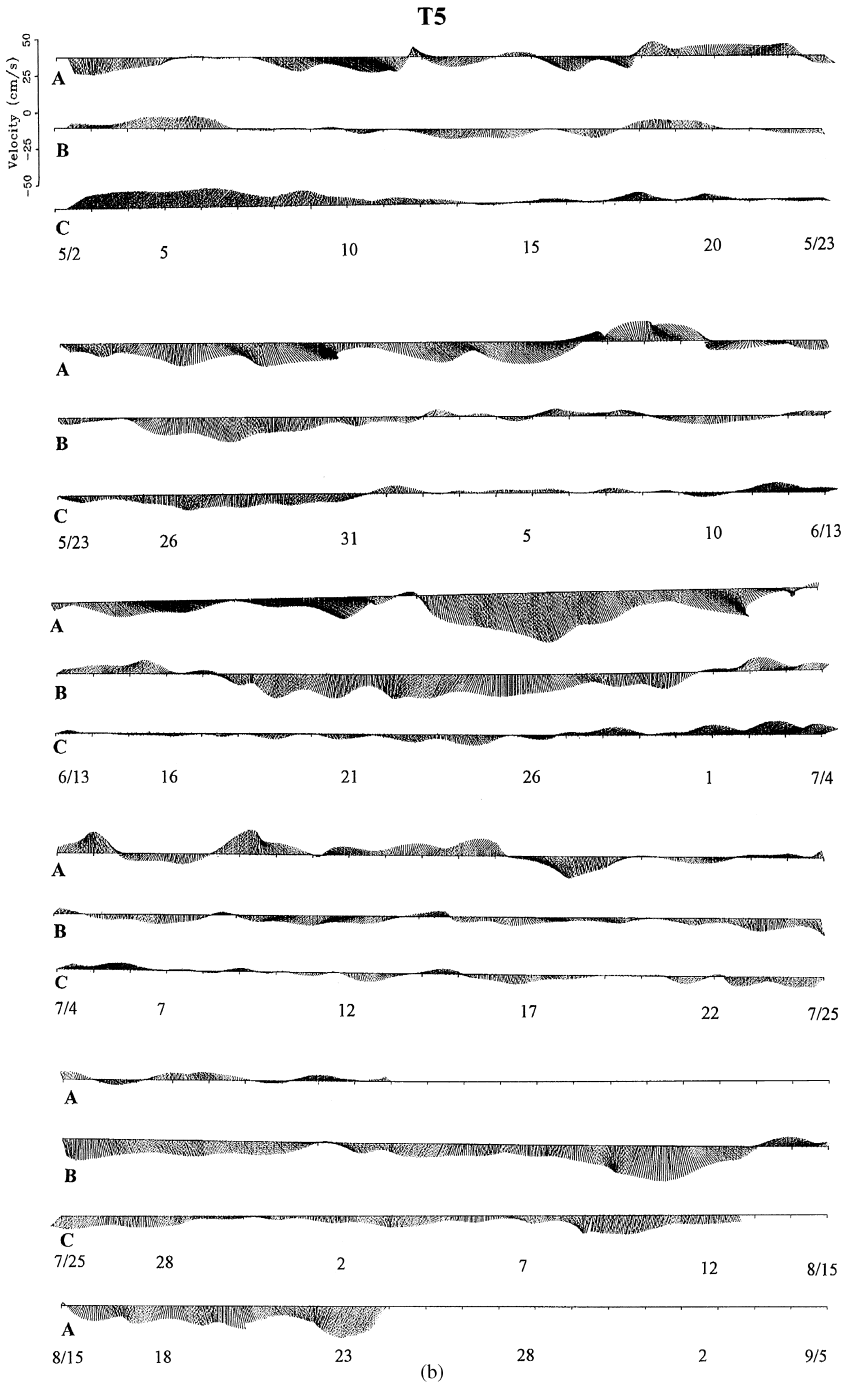

(b)

Fig. 7. (*Continued.*)

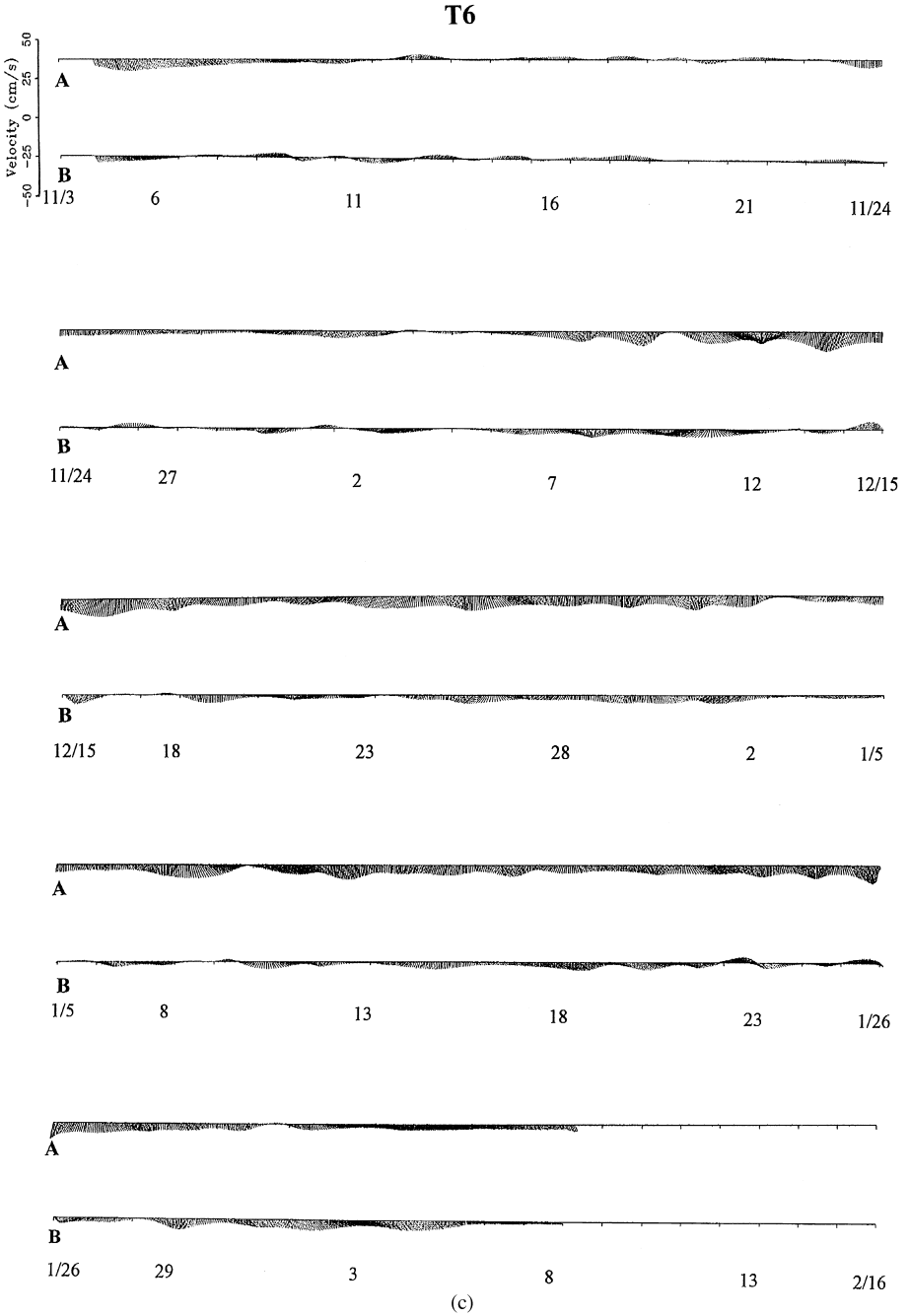

(c)

Fig. 7. (*Continued.*)

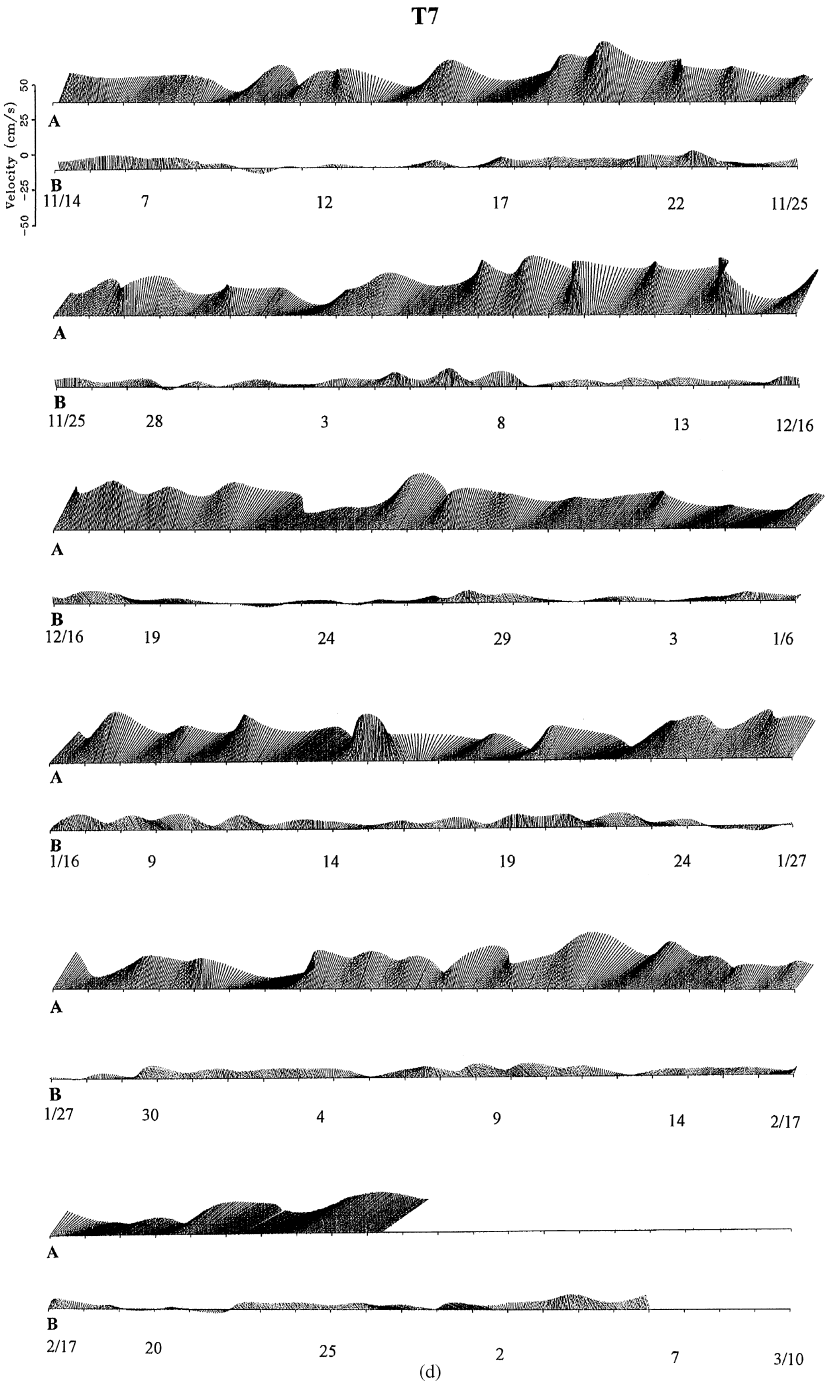

Fig. 7. (*Continued*.)

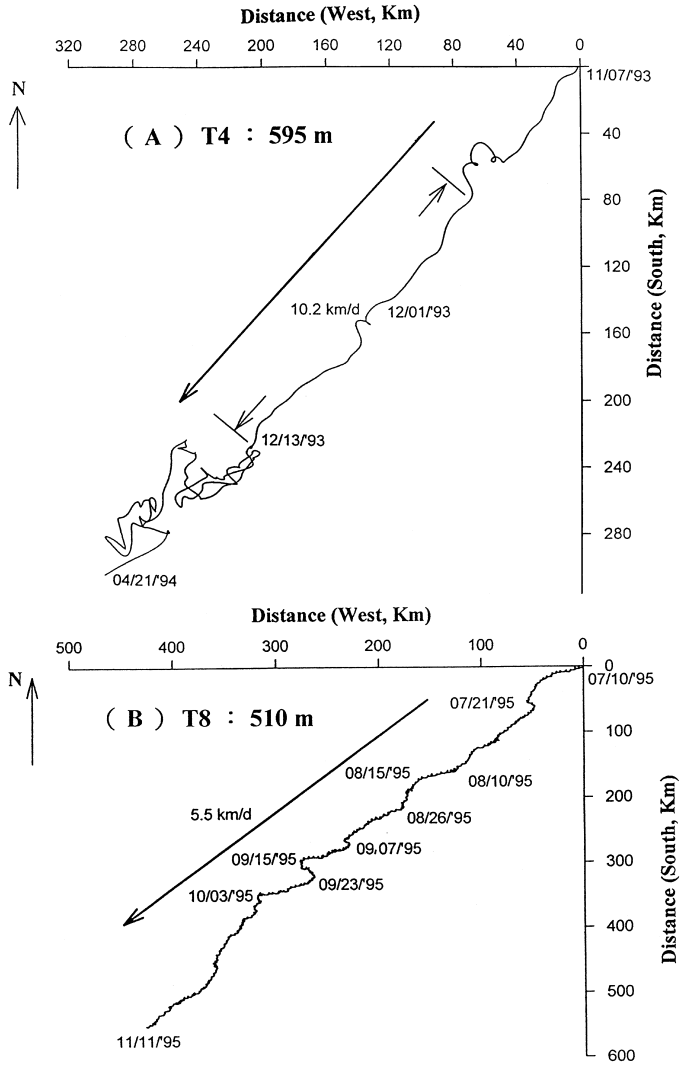

Fig. 8. Progressive vector diagram (PVD) showing a prevailing southwest flow at T4, 595 m (A) and T8, 510 m (B). Note the differences in scale between (A) and (B) as well as between the N–S and E–W axes in (B). Both PVDs indicate a southwest flow but the speed at T4 is about twice as fast as that at T8.

4. Discussion

The temporal variation in particulate flux at T1 in the Mien-Hua Canyon with a collection interval of 3 d was found to have good correlation with the associated tidal current oscillation, i.e. high mass flux occurred when the oscillation was large in amplitude (Hung and Chung, 1998). However, the other two sites (T2 and T3) in the

canyon showed no such correlation (Fig. 9). The E–W and N–S components of the tidal (unfiltered) currents were not correlated with the corresponding particulate fluxes as shown at the deepest traps from T2 (Fig. 9a) and T3 (Fig. 9b). The tidal current velocity oscillation is quite similar in pattern between T2 and T3, showing dominance of the E–W component over the N–S component. Thus, the deep tidal currents were mainly oscillating along the canyon axis. The oscillation amplitude was greater at T3 ($\sim \pm 50$ cm s^{-1}) than at T2 ($\sim \pm 30$ cm s^{-1}). At T3, each "quiet" period with small amplitude oscillation was shorter (about 4 d or less, much shorter than the trap collection time which was 8 d for each cup) than the time interval between two quiet periods (about 10 d or longer) based on the E–W velocity oscillation (Fig. 9b). At

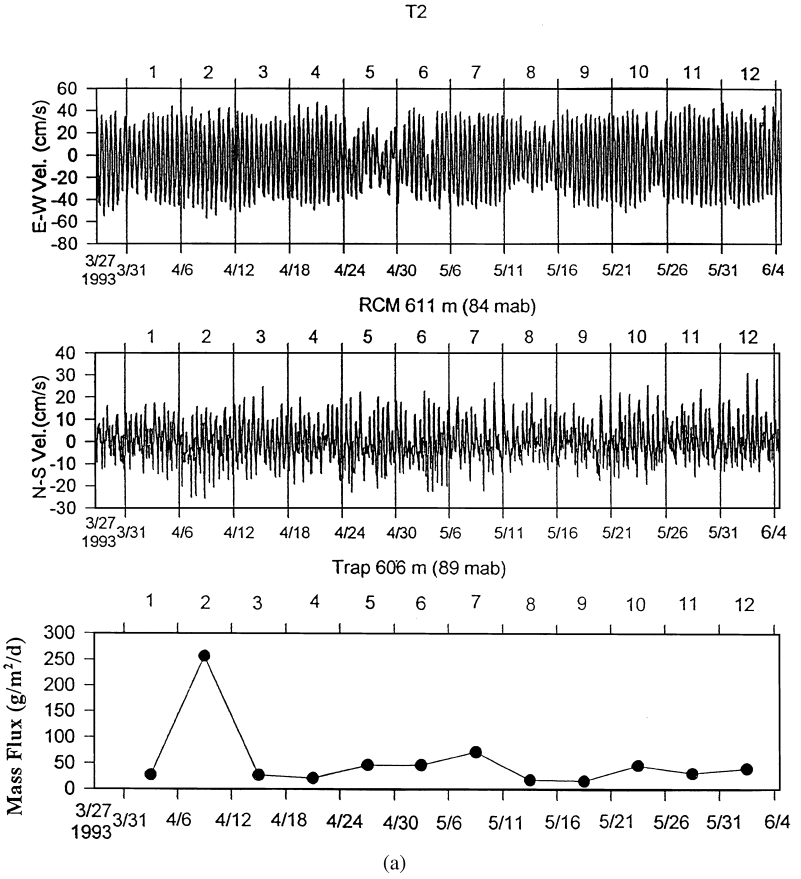

(a)

Fig. 9. Comparisons of the time-series current velocities in E–W and N–S components with the associated mass fluxes at T2 (611, 606 m) (a) and T3 (533, 528 m) (b). The collection cups of a trap are labelled sequentially with its starting time at the midnight (zero o'clock) of the indicated date in local time. No temporal correlations between the mass fluxes and the tidal current oscillations were observed at T2 and T3. The unusually high mass fluxes (T2: cup #2; T3: cups #4, 12) were probably due to episodic events unrelated to the currents.

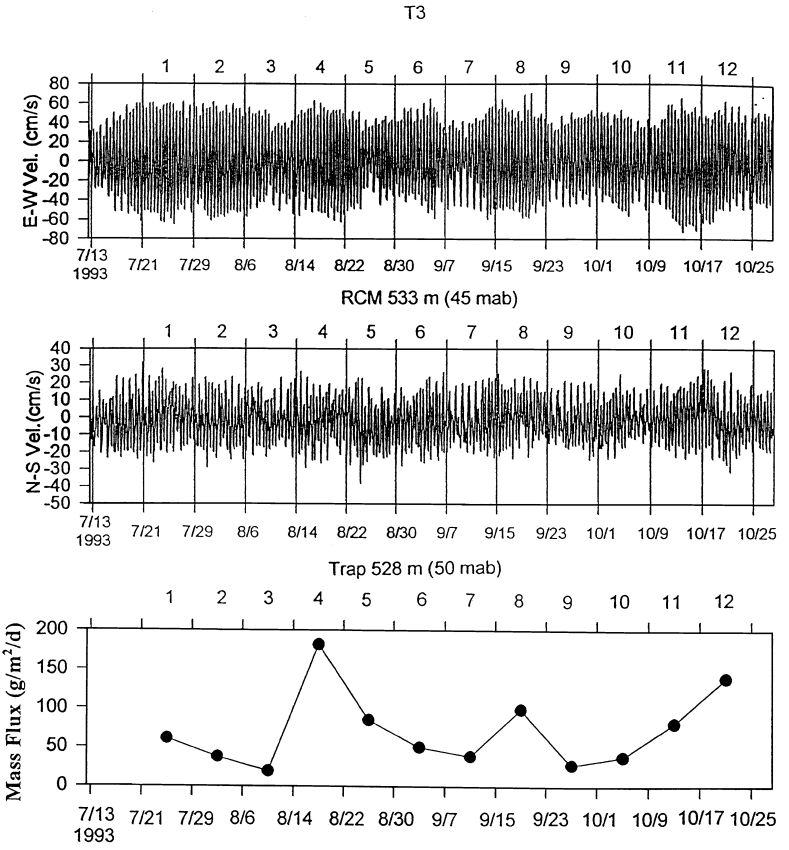

(b)

Fig. 9. (*Continued.*)

T2, the quiet periods appeared longer, up to 6 d, about the same as the collection time of each cup, e.g. cups #5 and #8 (Fig. 9a).

The extremely high mass flux of about 250 g m^{-2} d^{-1} collected at T2, cup #2 (4/6/1993–4/11/1993) was not correlated with any unusually strong tidal current at the same period; periods of relatively strong tidal currents were not necessarily associated with high mass fluxes (Fig. 9a). At T3, very high mass fluxes collected in cups #4, #8 and #12 were associated with periods of large tidal oscillation, but lower mass fluxes were collected in cups #1 and #2 although these two cups also corresponded to periods of large tidal oscillation (Fig. 9b). These observations suggest that the extremely high mass fluxes were not related to tidal currents. They were due to episodic events such as slumping which could have occurred earlier near the canyon head. The sand content in these high-flux samples was usually very high (e.g. > 70% for T2, cup #2; > 50% for T3, cup #4; see Hung and Chung, 1998). These samples contained about 90% lithogenic components but remained quite similar to other

Table 3
Prevailing direction and mean speed estimation from the current meter data

Site	Depth (m)	Prevailing direction	Mean speed ($cm\ s^{-1}$)	Period
T1	330	SWW	5	10/24/1992–11/8/1992
	412	NW	5	10/24/1992–12/3/1992
T2	409	NE	7	3/27/1993–6/2/1993
	611	W	5	3/27/1993–6/11/1993
T3	328	SW	10	7/12/1993–10/27/1993
	533	SW	5	7/12/1993–10/27/1993
T4	395	SES	20	11/7/1993–1/29/1994
	595	SW	10	11/7/1993–2/21/1994
T5	365	SE	15	5/2/1994–8/2/1994
	565	S	10	5/2/1994–8/26/1994
	765	E,S	5	5/2/1994–8/14/1994
	965	–[a]	5	5/2/1994–9/19/1994
T6	896	S	5	11/3/1994–2/10/1995
	1196	SE	3	11/3/1994–2/9/1995
T7	305	NE	30	11/4/1994–2/28/1995
	650	N	10	11/4/1994–3/8/1995
T8	360	–	5	7/10/1995–12/5/1995
	510	SW	7	7/10/1995–11/11/1995
T9	412	SWS	12	7/11/1995–12/23/1995
	512	SWS	8	7/11/1995–12/15/1995
T10	611	SW	5	7/10/1995–12/5/1995
	911	SWW	3	7/10/1995–11/27/1995

[a]–: No prevailing direction.

samples (Lin, 1997). Strong tidal currents with high kinetic energy could have kept these particulates suspended long enough to allow for lateral transport (Gardner, 1989a,b). However, resuspension was not necessarily responsible as a source for these particulates because large deficiency of ^{210}Po relative to ^{210}Pb was generally observed (Hung and Chung, 1998).

The low-pass filtered time-series current meter data expressed in stick diagrams and progressive vector diagrams (e.g. Figs. 7 and 8) allow us to estimate the prevailing direction and mean speed of the net flow at each moored site and depth during the mooring period. The results are summarized in Table 3 which also indicated the period for each mooring. The mean speed varied from 3 to 30 $cm\ s^{-1}$, but most values were about 5 to 10 $cm\ s^{-1}$. The maximum value observed at T7 was due to the Kuroshio which intrudes northward while flows northeastward at this site. The current meter was located at 305 m depth, but the upper trap was 200 m below and thus much lower values ($\sim 10\ cm\ s^{-1}$ at 650 m. Table 3) were expected. Therefore, it seems unlikely that the low mass fluxes measured from T7 were due to low trapping efficiency caused by strong current (Baker et al., 1988). Recently, Gardner et al. (1997) showed that even variable horizontal flows and associated fluxes at the Vema Channel had little effect on measured vertical fluxes within the channel.

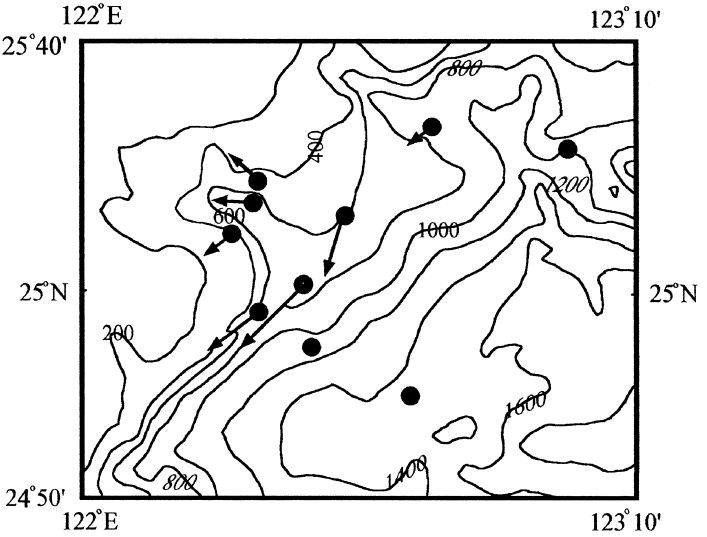

Fig. 10. Prevailing current velocities at 5 m below the deepest traps (50–100 mab) compiled from the current meter data. A general southwest flow along the isobaths between 500 and 800 m is indicated near the outlet of the Mien-Hua Canyon. Refer to Fig. 1 for mooring sites identification.

Along the isobaths at about 500 m depth and below (T4, T8 and T9, see Fig. 1), the currents were mostly toward the southwest at a moderate speed (less than 10 cm s^{-1}) even though data were compiled from different seasons with variable length of mooring time. This is illustrated in Fig. 10 which shows the flow pattern and speed at the sites where current meter data indicate a prevailing direction within the bottom 100 m layer. At T6 near the South Okinawa Trough, the flow at 1196 m depth (250 mab) assumed a somewhat random pattern with a weak south or southeast flow (Table 3). The flow pattern shown in Fig. 10 is quite different from that observed above 300 m depth by ADCP (Tang and Yang, 1994; Tang et al., 2000). Above 300 m depth, the currents were heading mostly toward the northeast, following the Kuroshio path, but also intruding onto the ECS shelf through the slope area between the North Mien-Hua Canyon and Mien-Hua Canyon (Tang et al., 2000).

The mass fluxes of the three size fractions (in terms of clay, silt and sand based on laser particle counting results) at T4–T6 are shown in Fig. 11 which indicates that silt dominates the particles trapped at these sites. An episodic event of high mass fluxes occurred at all depths at T4 during cups #6 and #7 collections. At T5, a similar event marked by high mass fluxes also occurred at all depths during cups #11 and #12 collections, a period of 20 d. No such event occurred at T6, a deep site with more uniform mass fluxes of mainly silt component, probably because the traps were located far and deep enough from the effect of any event. Within the Mien-Hua Canyon, the major components collected from T1 to T3 were silt and sand (Hung and Chung, 1998). The silt and sand fractions were responsible for the very high mass fluxes observed in the canyon. Since less particulates were trapped at T4–T6 sites than

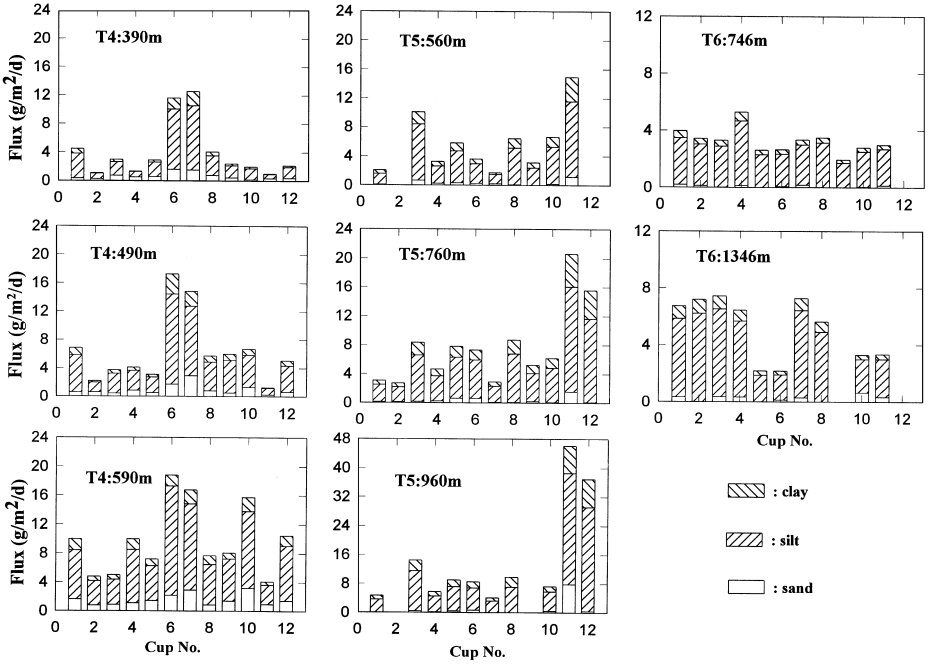

Fig. 11. Mass fluxes of clay, silt and sand fractions from T4 to T6. Different scales are used to accommodate a large range of the flux values. A few samples from T5 and T6 were not analyzed due to limited quantity of the samples. Some episodic events of relatively high fluxes with large components of silt and sand occurred at T4 and T5. More uniform fluxes with mostly silt were observed at T6, which was located closest to the South Okinawa Trough.

at the canyon sites, most of the particulates were not transported directly from the canyon toward the trough. Based on the flow pattern compiled from the current meter data (Fig. 10), these particulates were most likely transported out of the canyon and then along the isobaths below 500 m depth of the slope toward the southwest.

In the Mien-Hua Canyon, high mass fluxes which were usually due to high sand fraction, were essentially associated with large tidal current oscillations (Hung and Chung, 1998). Beyond the canyon, the mass fluxes observed at T4–T6 were substantially lower with less sand fraction. Fig. 12 shows plots of sand content in percent vs. mass flux for each individual trap sample collected from T1 to T6. Two distinct groups are marked by two different symbols. The data from T1 to T3 show that high mass fluxes are often associated with high sand contents while those from T4 to T6 show that lower mass fluxes are accompanied by lower sand contents. Hung and Chung (1998) calculated the time-averaged fractions of sand, silt and clay for each trap from T1 to T3. The results showed that the sand fraction was about 21–35%, the silt fraction 55–61%, and the clay fraction 10–15%. However, the surface sediments collected nearby showed large variations: on the shelf or shelf break, sand and gravel were major components because fine-grained sediments might have been resuspended

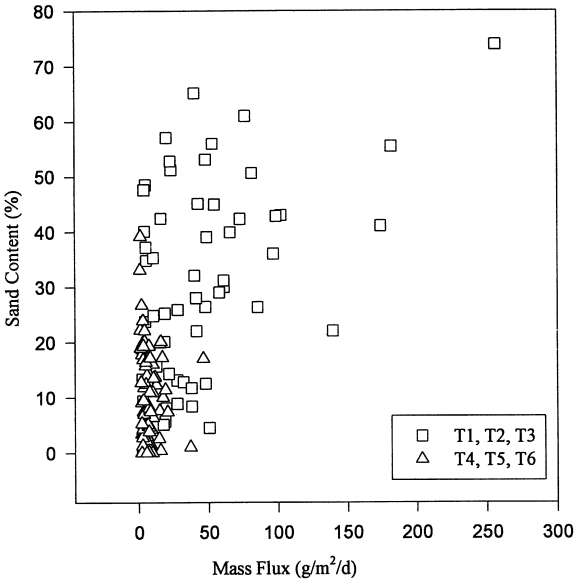

Fig. 12. Plots of sand content in percent vs. mass flux for the Mien-Hua canyon sites (T1–T3), and the slope sites extending out of the canyon (T4–T6). High mass fluxes with high sand contents were generally observed in the canyon while lower fluxes with lower sand contents were noted in the slope area. While the canyon data scatter over a large domain in both sand content (5–70%) and mass flux (5–250 g m^{-2} d^{-1}), the slope data cluster in a small range of flux (< 50 g m^{-2} d^{-1}) and of sand content (< 40%).

and transported away (Baker and Hickey, 1986; Hickey et al., 1986); in the canyon or lower slope, silt and clay were of equal importance perhaps due to lack of resuspension. The clay content was much higher (45–60%) in the lower slope sediments than in the particulates trapped above the area nearby. This suggests that the particulates were transported laterally from the canyon head and/or shelf zone through the canyon with little settling, and that the clay in sediments was accumulated probably over a long period without being perturbed.

The particulate matter in the study area was also collected by filtering seawater samples and weighing to determine its concentration distribution by other KEEP investigators (Hung and Chan, 1998; Hung et al., 2000). A NW–SE transect extending from the shelf to the slope was surveyed in April, 1992. The results showed that the particulate matter concentration (PMC) was extremely high near shore (4.2 mg l^{-1}), and decreased toward the outer southern ECS shelf (about 0.7–1.5 mg l^{-1}, Hung and Chan, 1998). From the shelf break via the slope to the South Okinawa Trough, the PMC decreased from 0.5 to 0.2 mg l^{-1} and was quite uniform vertically at about 0.4 mg l^{-1} near the upwelling cold dome. In winter (November, 1994) the PMC was about 0.3 mg l^{-1} (Hung et al., 2000) due to lower particulate organic carbon (POC) content resulting from lower productivity. The POC content in percent of the filtered particulates increased toward the open ocean mainly because the terrestrial material had decreased substantially. While the POC in the trapped particulates was usually

about 2% or less (Lin, 1997), the filtered POC ranged from about 5% near the bottom to above 30% in the surface water (Hung et al., 2000). The large difference in relative abundance of POC observed between the two sampling methods suggests that a very large portion of POC was not settling and thus not collected by traps.

The mean PMC in the slope area was about 0.4 mg l^{-1} as determined by filtration (Hung and Chan, 1998; Hung et al., 2000). If we assume that this PMC contained about 15% POC or 30% particulate organic matter (POM), then about 70% or 0.3 mg l^{-1} of PMC was terrigenous or lithogenic materials. The mean mass flux in the same slope area was about 10 g m^{-2} d^{-1} (T4–T6). Neglecting the POM portion ($\sim$ 5%), we obtained a mean settling rate of about 30 m d^{-1}. With a mean depth of about 1000 m at these sites, the mean particulate settling time was only 30 d or a month. At a mean flow speed of 6–10 km d^{-1} (Fig. 8), these particulates could be transported laterally for about 180–300 km, far enough to reach the deep South Okinawa Trough even though the pathway was along the isobaths toward the west end of the trough before heading east to the trough, as indicated by the current meter data (Fig. 10).

5. Conclusions

The apparent mass fluxes at each mooring site increased with depth and the time-series variations were cyclic and well synchronized at the same site for some sites. However, the associated current meter data (Fig. 7) showed no similar cyclic or synchronized variations. The particulate fluxes within the Mien-Hua Canyon showed a pronounced increase toward the bottom but those from the other sites on the slope between the southern ECS shelf and the South Okinawa Trough increased only moderately or slightly with depth. High mass fluxes and large increases with depth in the bottom 200 m layer within the canyon implied that the particulates were mainly transported from the shelf break along the canyon within this layer. The particulate fluxes measured in the general slope area were much lower and the values decreased toward the South Okinawa Trough. This pattern of mass flux variations suggests that most particulates on the shelf or shelf break were transported to the deep sea preferentially through canyons, not over the general slope area.

The major components of the trap samples in the canyon were silt and sand (Hung and Chung, 1998), but those on the slope were mainly silt (Fig. 11). These sand and silt components were of terrigenous origin. Both the sand contents and mass fluxes were high in the canyon but much lower in the slope area (Fig. 12). A large portion of the particulates collected by traps in the canyon was probably transported along the isobaths or topographic contours from the canyon outlet toward the southwest rather than directly into the trough based on the high mass fluxes observed at T8 and the available current meter data (Figs. 7, 8 and 10). The relatively low mass fluxes observed at T7 near the outlet of the North Mien-Hua Canyon where a branch of the Kuroshio intrudes onto the ECS shelf suggest that the Kuroshio water is quite "clean" in terms of particle loading. The currents observed at depths where sediment traps were deployed were generally weaker than those above 300 m depth, and the

circulation patterns were also quite different (Tang and Yang, 1994; Tang et al., 2000). A simple calculation suggests that the mean particulate settling time is about 30 d in a water column of 1000 m depth. This mean settling time is long enough for the particulates to be transported into the South Okinawa Trough based on the current meter data (Table 3 and Figs. 7, 8 and 10).

Acknowledgements

The financial support for this study was provided over the past years by the National Science Council (NSC), Taiwan, Republic of China, under grants: NSC 82-0209-M-110-043K, NSC 83-0209-M-110-011K, NSC 84-2611-M-110-002-K2 and NSC 85-2611-M-110-007-K2. The authors wish to thank the marine technicians, research assistants and crews aboard the R/V *Ocean Researchers* I and II for their help during the deployments and recoveries of the sediment traps. Professor T.Y. Tang of National Taiwan University has provided valuable assistance with the current meter data handling and discussion on the interpretation of these data. Assistance by C.N. Chen in many aspects of this research is much appreciated. L.C. Hung, C.W. Peng and H.C. Chang have typed the manuscript and prepared the figures.

References

Baker, E.T., Hickey, B.M., 1986. Contemporary sedimentation processes in and around an active west coast submarine canyon. Marine Geology 71, 15–34.

Baker, E.T., Milburn, H.B., Tennant, D.A., 1988. Field assessment of sediment trap efficiency under varying flow conditions. Journal of Marine Research 46, 573–592.

Biscaye, P.E., Anderson, R.F., 1994. Fluxes of particulate matter on the slope of the southern Middle Atlantic Bight: SEEP-II. Deep-Sea Research II 41, 459–509.

Biscaye, P.E., Anderson, R.F., Deck, B.L., 1988. Fluxes of particles and constituents to the eastern United States continental slope and rise: SEEP-I. Continental Shelf Research 8, 855–904.

Chao, S.-Y., 1990. Circulation of the East China Sea, a numerical study. Journal of the Oceanographic Society of Japan 46, 273–295.

Chern, C.-S., Wang, J., 1990. The exchange of Kuroshio and East China Sea shelf water. Journal of Geophysical Research 95, 16,017–16,023.

Chuang, W.-S., Wu, C.K., 1992. Slope current fluctuations northeast of Taiwan, winter 1990. Journal of the Oceanographic Society of Japan 47, 185–193.

DeMaster, D.J., McKee, B.A., Nittrouer, C.A., Qian, J., Cheng, G., 1985. Rates of sediment accumulation and particle reworking based on radiochemical measurements from continental shelf deposits in the East China Sea. Continental Shelf Research 4, 143–158.

Fan, K.L., 1980. On upwelling off northeastern shore of Taiwan. Acta Oceanographica Taiwanica 11, 105–117.

Gardner, W.D., 1989a. Baltimore Canyon as a modern conduit of sediment to the deep sea. Deep-Sea Research 36, 323–358.

Gardner, W.D., 1989b. Periodic resuspension in Baltimore Canyon by focusing of internal waves. Journal of Geophysical Research 94, 18,185–18,194.

Gardner, W.D., Biscaye, P.E., Richardson, M.J., 1997. A sediment trap experiment in the Vema Channel to evaluate the effect of horizontal particle fluxes on measured vertical fluxes. Journal of Marine Research 55, 995–1028.

Heussner, S., Ratti, C., Carbonne, J., 1990. The PPS 3 time-series sediment trap and the trap sample processing techniques used during the ECOMARGE experiment. Continental Shelf Research 10, 943–958.

Hickey, B., Baker, E., Kachel, N., 1986. Suspended particle movement in and around Quinault Submarine Canyon. Marine Geology 71, 35–83.

Hung, G.W., Chung, Y., 1998. Particulate fluxes, ^{210}Pb and ^{210}Po measured from sediment trap samples in a canyon off northeastern Taiwan. Continental Shelf Research 18, 1475–1491.

Hung, J.J., Chan, C.L., 1998. Distribution and enrichment of particulate trace metals in the southern East China Sea. Geochemical Journal 32, 189–203.

Hung, J.J., Lin, P.L., Liu, K.K., 2000. Dissolved and particulate organic carbon in the southern East China Sea. Continental Shelf Research 20, 545–569.

Lin, C.S., 1997. Fluxes of particles and chemical constituents in the southern East China Sea northeast of Taiwan. M.S. Thesis, National Sun Yatsen University, Kaohsiung (in Chinese).

Liu, K.K., Gong, G.C., Shyu, C.T., Pai, S.C., Wei, C.L., Chao, S.Y., 1992. Response of Kuroshio upwelling to the onset of northeast monsoon in the sea north of Taiwan: observations and a numerical simulation. Journal of Geophysical Research 97, 12511–12526.

Monaco, A., Courp, T., Heussner, S., Carbonne, J., Fowler, S.W., Deniaux, B., 1990. Seasonality and composition of particulate fluxes during ECOMARGE-I, western Gulf of Lions. Continental Shelf Research 10, 959–987.

Sheu, D.D., Jou, W.C., Chung, Y.C., Tang, T.Y., Hung, J.J., 1999. Geochemical and carbon isotopic characterization of particles collected in sediment traps from the East Chine Sea continental slope and the Okinawa Trough northeast of Taiwan. Continental Shelf Research 19, 183–203.

Tang, T.Y., Tang, W.T., 1994. Current on the edge of the continental shelf northeast of Taiwan. Terrestrial Atmospheric and Oceanic Sciences (TAO) 5, 335–348.

Tang, T.Y., Tai, J.H., Yang, Y.T., 2000. The flow pattern north of Taiwan and the migration of the Kuroshio. Continental Shelf Research 20, 349–371.

Tang, T.Y., Yang, Y.J., 1994. ADCP I-V Data Report. Institute of Oceanography, National Taiwan University (in Chinese).

Wong, G.T.F., Pai, S.C., Liu, K.K., Liu, C.T., Chen, C.T.A., 1991. Variability of the chemical hydrography at the frontal region between the East China Sea and the Kuroshio northeast of Taiwan. Estuarine, Coastal and Shelf Science 33, 105–120.